Dopamine signaling modulates the stability and integration of intrinsic brain networks

Golia Shafiei,[1] Yashar Zeighami,[1] Crystal A. Clark,[1] Jennifer T. Coull,[2,3] Atsuko Nagano-Saito,[1,4,5] Marco Leyton,[1,5] Alain Dagher,[1] and Bratislav Mišić[1,*]

[1] *Montréal Neurological Institute, McGill University, Montréal, Canada*
[2] *Laboratoire des Neurosciences Cognitives UMR 7291, Federation 3C, Aix-Marseille University, France*
[3] *Centre National de la Recherche Scientifique (CNRS), Paris, France*
[4] *Centre de Recherche, Institut Universitaire de Gériatrie de Montréal, Montréal, Canada*
[5] *Department of Psychiatry, McGill University, Montréal, Canada*

(Dated: January 31, 2018)

Dopaminergic projections are hypothesized to stabilize neural signaling and neural representations, but how they shape local information processing and large-scale network interactions remains unclear. Here we investigated the effects of lowered dopamine levels on functional connectivity and signal variability in the healthy brain at rest. The acute phenylalanine and tyrosine depletion (APTD) method was used to decrease dopamine synthesis in 51 healthy participants who underwent high-resolution resting-state functional MRI (fMRI). Functional connectivity and regional signal variability were estimated for each participant. Multivariate partial least squares (PLS) analysis was used to statistically assess changes in signal variability following APTD as compared to the balanced control treatment. The analysis captured a pattern of increased signal variability following dopamine depletion. Changes in signal variability were concomitant with changes in functional connectivity, such that nodes with the greatest increase in signal variability following dopamine depletion also experienced the greatest decrease in functional connectivity. Our results suggest that dopamine may act to stabilize neural signaling, particularly in networks related to motor function and orienting attention towards behaviorally-relevant stimuli. Moreover, dopamine-dependent signal variability is critically associated with the functional embedding of individual areas in large-scale networks.

INTRODUCTION

The brain is a complex network of interacting neuronal populations that collectively support perception, cognition and action. Transient episodes of synchrony establish brief windows for communication among remote neuronal populations [26], manifesting as patterns of functional connectivity and large-scale resting state networks [60, 78]. Thus, regional neural activity reflects computations that result from network interactions, but also drives those interactions [20]. How the balance between local dynamics and global functional interactions (connectivity) is modulated remains unclear.

Dopamine is thought to stabilize neuronal signaling by modulating synaptic activity and signal gain [69]. Dopamine, acting in cortex or striatum, could regulate cortical representations by facilitating or suppressing neural signaling. These effects may also play a role in reinforcement learning, based on the theory of dopaminergic reward prediction error signaling [67]. In humans, transient decreases in dopamine synthesis (which we term as *"dopamine depletion"* throughout this manuscript) have been shown to disrupt multiple aspects of perception, motor control and executive function, [18, 56, 57, 61], consistent with a role in the regulation of sustained cortical activity [69]. Similar effects have also been demonstrated in various animal models including rodents and monkeys [68]. Furthermore, the death of dopamine neurons in Parkinson's disease (PD) leads to unstable and increasingly variable motor output [9, 43]. By stabilizing neuronal signaling, dopamine may thus influence the stability of regional activity and its potential for functional interactions at a network level.

Here we use resting-state functional magnetic resonance imaging (fMRI) to investigate the effects of dopamine depletion on local signal variability and intrinsic brain networks. We applied acute phenylalanine and tyrosine depletion (APTD) to transiently decrease dopamine levels in healthy participants [16, 41, 42, 48, 55, 59]. We hypothesized that dopamine depletion would destabilize regional activity, manifesting as increased signal variability. We further hypothesized that regions with increased signal variability may be less likely to interact with other regions, resulting in decreased functional connectivity.

RESULTS

Task-free, resting-state fMRI was recorded in $n = 51$ healthy young participants on two separate days, once following administration of a nutritionally balanced amino acid mixture (BAL) and once following acute phenylalanine/tyrosine depletion (APTD). Anatomical MRI data were parcelled into five progressively finer resolutions, comprising 83, 129, 234, 463 and 1015 nodes [15]), which were used for extraction of blood-oxygen-level dependent (BOLD) time series. We investigated how dopamine depletion affects (a) local, region-level ac-

* Corresponding Author: bratislav.misic@mcgill.ca

tivity, (b) global, between-region functional connectivity and (c) the relationship between the two.

Dopamine depletion increases signal variability

We estimated regional signal variability using sample entropy (SE), a measure of the unpredictability of a time series [62]. Briefly, the SE algorithm quantifies the conditional probability that any two sequences of $m+1$ time points will be similar to each other given that the first m points were similar (Fig. S1). We then used multivariate partial least squares (PLS) analysis to statistically assess changes in signal variability following administration of the BAL vs. APTD mixtures [46]. PLS results in a set of latent variables (LV), that are weighted combinations of experimental design (i.e., a contrast) and signal variability patterns that optimally covary with each other.

The analysis revealed a single statistically significant latent variable (permuted $p = 0.014$ for the finest parcellation resolution with 1015 nodes), showing broadly increased signal variability following dopamine depletion (Figure 1). Bootstrap resampling was used to estimate the reliability with which individual nodes contribute to the overall multivariate pattern. Specifically, the weight or loading associated with each node was divided by its bootstrap-estimated standard error, yielding a measure ("bootstrap ratio") that is high for nodes with large weights (i.e., large contributions) and small standard errors (i.e., are stable) [45]. Note that bootstrap ratios may be interpreted as z-scores if the sampling distribution is approximately unit normal [25]. Positive bootstrap ratios indicate an increase in signal variability, while negative bootstrap ratios indicate decreased variability. Figure 1b depicts a brain projection of this statistical pattern, showing that the greatest increase in signal variability was observed in somatomotor cortex. This effect (increased variability following depletion) and the spatial pattern were consistent across all five spatial resolutions (Figure S2).

Increased signal variability in somatomotor and salience networks

We next investigated the effect of APTD on resting state networks [60, 78]. Figure 2a depicts the nodes displaying the greatest increase in signal variability following dopamine depletion in descending order and colour-coded by resting state network membership [52]. The most affected nodes appear to belong primarily to the somatomotor (yellow) and salience (green) networks suggesting that the signal variability may selectively affect certain large-scale networks.

To further address the network-selectivity of dopamine depletion, we first estimated the mean change in signal variability across all nodes in a given network, using PLS-derived bootstrap ratios for the finest resolution (1015 nodes). To determine which network-level changes were statistically significant and not due to differences in network size, spatial contiguity or lateralization, we randomly permuted network labels within each hemisphere and recomputed network means 10,000 times, generating a distribution under the null hypothesis that network assignment does not influence the overall change in signal variability. A p-value was estimated for each network as the proportion of times when the mean for the permuted network assignment exceeded the mean for the original empirical network assignment. Figure 2b shows that increases and decreases in signal variability were observed for all intrinsic networks, but that increased variability was greatest and statistically significant for the somatomotor ($p \approx 0$) and salience networks ($p = 10^{-4}$).

To ensure that these results are independent of how intrinsic networks are defined, we repeated the procedure using partitions reported by Yeo and colleagues [78] and by Power and colleagues [60] (Figure S4). The results were consistent across the three partitions, indicating significant increased signal variability in somatomotor and ventral attention networks among Yeo networks (note that the 'ventral attention network' overlaps with the 'salience network' shown in Figure 2), and in somatosensory and auditory networks among Power networks. No significant decrease in signal variability was observed in any intrinsic networks, regardless of which network assignments were used.

Increased signal variability correlates with decreased functional connectivity

Given that changes in signal variability were highly network dependent, we next investigated whether increased signal variability is related to patterns of functional connectivity. Functional connectivity was estimated as a Pearson correlation coefficient between regional time series for each participant in each condition. To relate patterns of signal variability with functional connectivity, we estimated a group-average functional connectivity matrix by calculating the mean connectivity of each pair of brain regions across all participants.

We observed a weak relationship between increased signal variability and decreased functional connectivity, such that nodes with the greatest increase in signal variability following dopamine depletion also experienced the greatest decrease in functional connectivity ($R^2 = 0.044$, $p = 1.59 \times 10^{-11}$; Figure 3a). We also compared the average functional connectivity across all nodes following the BAL vs. APTD conditions and identified a weak but statistically significant overall decrease after APTD ($p = 0.01$; Wilcoxon rank sum test, one-tailed; Figure 3b). Although significant, both effects were small, suggesting that the relationship was not sustained over the bulk of data points (nodes), but that it may have been driven by a subset of these points instead.

To investigate this possibility, we assessed dopamine-

dependent changes in functional connectivity in each of the intrinsic networks separately. Overall, functional connectivity decreased in only two of the original networks: somatomotor and salience ($p = 0.002$ and $p = 0.023$ respectively; Wilcoxon rank sum test, one-tailed; Figure 3b). Critically, these were the two networks that also experienced the greatest increase in signal variability after APTD (Figure 2). Overall, these results suggest that the effects of dopamine depletion are selective and localized to specific large-scale systems. Moreover, these changes in local dynamics are related to global functional interactions.

Selective disconnection of intrinsic networks

Dopamine-related increases in signal variability appear to be concomitant with decreased functional connectivity localized to specific intrinsic networks. However, it is unclear whether decreased connectivity in the somatomotor and salience networks is driven by weakened within-network or between-network connections, or both.

To address this question, we calculated the participation coefficient and within-module degree z-score of every node [33]. The participation coefficient quantifies the diversity of a node's connectivity profile. A participation coefficient with a value close to 1 indicates that a node's connections are evenly distributed across communities, while a value close to 0 indicates that most of the node's connections are within its own community. The within-module degree z-score of a node is a normalized measure of the strength of connections a node makes within its own community.

Figure 4 shows that the participation coefficient significantly decreases in somatomotor, salience and ventral attention networks following dopamine depletion ($p = 6.18 \times 10^{-7}$, $p = 0.005$ and $p = 0.005$ respectively), while the within-module degree z-score does not. In other words, dopamine depletion selectively reduced functional interactions between these networks and the rest of the brain (participation coefficient; Figure 4, top), but did not affect within-network cohesion (within-module degree z-score; Figure 4, bottom). Overall, these results suggest that dopamine depletion effectively segregates these networks from the rest of the brain. Note that the three networks with significant decreases in participation coefficient are the ones with maximum increases in signal variability.

We also investigated average changes in participation coefficient and within-module degree z-score in other intrinsic networks, where we did not observe any significant changes in either of the two measures (Figure S5). In addition, we estimated the average within- and between-module connectivity across all nodes following the BAL vs. APTD conditions. Confirming the previous results, we observed a significant decrease in between-module connectivity in somatomotor, salience and ventral attention networks following APTD ($p = 0.001$, $p = 0.027$ and $p = 0.032$ respectively) while there was no significant difference observed in within-module connectivity (Figure S5).

No systematic effect of study

The data used in this study were consolidated from three different experiments [18, 56, 57], so it is possible that the observed effects were idiosyncratic to one or two of the constituent datasets and do not necessarily generalize across all three studies. To investigate this possibility, we used a multi-way ANOVA to assess differences between studies: subject-specific scores were calculated for the signal variability pattern and the three studies were treated as separate groups. The analysis did not reveal any significant difference among the three studies ($F(2, 45) = 1.7$, $p = 0.19$), nor any condition by study interaction ($F(2, 45) = 0.68$, $p = 0.51$). There was a significant condition difference, with greater scores in the depletion versus non-depletion condition ($F(1, 45) = 131.06$, $p \approx 0$), but this is expected given that the scores were derived by PLS to maximize this condition difference.

DISCUSSION

We investigated the effect of dopamine depletion on the balance between local node properties and global network architecture. We report two key results: (1) dopamine depletion selectively destabilizes neural signaling in salience and somatomotor networks, and (2) increased local variability in these intrinsic networks is accompanied by their disconnection from the global functional architecture. Altogether, these results point to a stabilizing influence of dopamine on neural signaling and highlight the link between local, node-level properties and global network architecture.

Linking local and global dynamics

The present results highlight the relationship between local signal variability and functional embedding. Increased variability in salience and somatomotor networks was concomitant with decreased functional connectivity with the rest of the brain. It is possible that low dopamine states disrupt local neuronal signaling, making it less likely for remote populations to synchronize. Alternatively, dopamine depletion may disrupt inter-regional synchrony through a separate mechanism, resulting in greater local variability. The correlative nature of the results cannot be used to disambiguate these two possibilities and further causal experiments are necessary. In any case, the present report demonstrates that functional interactions span multiple topological scales, such that local and global dynamical properties cannot be fully appreciated in isolation [11, 13].

Interestingly, dopamine depletion reduced between-module connectivity but did not affect within-module connectivity (Figure 4 and Figure S5). The effect was highly specific: reduced between-module connectivity was observed only in networks that also experienced increased signal variability. In other words, dopamine depletion affected how nodes within these networks communicated with the rest of the brain, but did not affect their internal cohesion. A recent study demonstrated a similar effect at the level of resting state networks: networks with greater temporal variability displayed greater within-network cohesion and lower between-network integration [40]. Altogether, these results suggest that functional network architecture shapes the relationship between local dynamics and global interactions.

Recent theories emphasize dynamic over static brain function. At the network level, reconfiguration of functional interactions is increasingly recognized as an informative attribute of healthy brain function and dysfunction [14]. Functional reconfiguration has been observed across multiple temporal scales, both at rest [8, 79] and with respect to a variety of cognitive functions [73], including learning [3, 53], attention [74] and working memory [36], and even conscious awareness [1, 31]. In parallel, the dynamic range of local signal fluctuations has emerged as a node-level marker of brain function [29, 63]. Traditionally disregarded as "noise", changes in signal variability have been reported across the lifespan [27, 34, 44], in multiple perceptual, cognitive and affective tasks [28, 51, 66] and in a variety of psychiatric and neurological diseases [7, 49, 50].

While most methods for estimating variability focus on node-level time series, several recent studies have conceptualized variability with respect to functional network embedding [50, 71]. For instance, local variability can be defined as the tendency for a node to switch network allegiance or to interact with multiple networks [12, 80]. This dynamic network switching is conditioned by an underlying anatomy [70, 80], but is also likely to be influenced by a variety of neurotransmitters. A prominent hypothesis is that dopamine modulates signal-to-noise ratio [54, 66]. We turn to the specific role of dopamine next.

Stabilizing influence of dopamine

Our results suggest that dopamine may act to stabilize neural signaling, particularly in networks associated with motor control (somatomotor network) and orienting attention towards behaviorally-relevant stimuli (salience network). Dopamine depletion was simultaneously associated with increased signal variability and decreased extrinsic connectivity, indicating that dopaminergic signaling influences both local information processing and network-wide interactions. Importantly, the effects of depletion were not confined to a single locus but distributed over two large-scale networks, suggesting that even temporary decreases in dopamine availability can disrupt local neuronal signaling and have far-reaching effects on synchrony among multiple systems.

A prominent hypothesis holds that dopamine modulates synaptic activity and signal gain [69]. Mechanistic studies *in vitro* have demonstrated that dopamine influences intrinsic ionic currents and synaptic conductance [23, 38]. These modulatory effects may facilitate or suppress neural signaling, helping to stabilize neural representations. In addition, dose-response effects of dopamine release may be both tonic and phasic [32], with the two modes thought to be mediated by distinct signaling pathways and receptors, and manifesting in distinct behavioural outcomes [19]. For instance, striatal medium spiny neurons of the direct pathway express D_1 receptors and are thought to promote movement and the selection of rewarding actions. Neurons in the indirect pathway mainly express D_2 receptors and are thought to inhibit cortical patterns that encode maladaptive or non-rewarding actions [76]. Although our results are consistent with the broad notion that dopamine stabilizes neural representations to facilitate reward learning and movement, further experiments are necessary to determine whether the observed effects can be attributed to tonic or phasic modulation.

Dopamine depletion can thus have local and global consequences, influencing a range of sensory-motor and higher cognitive functions. Age-related decline in dopaminergic transmission is hypothesized to lead to greater signal variability, influencing the distinctiveness of neural representations and, ultimately, performance [54, 66]. The stabilizing role of dopamine can also be observed in diseases associated with dopaminergic dysfunction, such as Parkinson's disease (PD), attention deficit hyperactivity disorder (ADHD) and schizophrenia. In PD for instance, cell death in substantia nigra leads to reduced dopaminergic transmission, with extensive motor symptoms. Intriguingly, dopamine depletion in PD is associated with reduced cortico-striatal functional connectivity patterns and reduced gait automaticity [30]. Similarly, in ADHD, reduced dopamine signaling is associated with deficits in goal-directed behaviour and reward learning [21].

Finally, the present results draw attention to an overlooked assumption of graph-based models of brain structure and function: that all nodes are identical, except for their connectivity patterns. In other words, graph representations often ignore important inter-regional differences that could influence neural activity and synchrony, including morphology, cytoarchitectonics, gene expression and receptor densities. How dopaminergic modulation interacts with modulation by other neurotransmitters is an exciting open question [72].

Methodological considerations

Our results may depend on a number of methodological choices and potential limitations, which we consider

in detail here. Methodological choices include the type of parcellation and resolution, intrinsic network definition, and parameter settings for SE. The reported effects are consistent across five resolutions (from 83 to 1015 nodes; Figure S2), three network partitions (detected using clustering, Infomap and Louvain methods; Figure S4) and a range of parameter settings (Figure S3). Although we took steps to mitigate concerns about these choices, the present results are based on a finite sampling of a multifactorial methodological space.

More generally, we studied the effects of dopamine depletion in the context of task-free, resting state fMRI, which presents two significant challenges for interpretation. First, dopaminergic transmission is inherently related to specific cognitive functions, which may be accessible without overt task demands. We find evidence that dopamine depeltion affects information transfer in two intrinsic networks with specific functional properties, but more research is necessary to investigate how dopamine affects the function of these networks in the presence of task demands. Second, dopaminergic transmission within specific subcortical and cortical circuits occurs at time scales that may be inaccessible with BOLD imaging. The present results can be used to draw conclusions about slow, modulatory effects of dopamine, but more electrophysiological evidence is necessary to relate these effects to faster phasic dopaminergic responses.

Summary

Our results support a link between local node dynamics and network architecture. Pharmacological perturbation may selectively target and disconnect specific networks without altering their internal cohesion. These results demonstrate that the stabilizing effect of dopamine on synaptic signaling extends to the level of large-scale brain networks.

MATERIALS AND METHODS

Participants

Altogether, $n = 51$ healthy young individuals (right-handed, 23.6 ± 5.9 years old, 32 men/19 women) participated in 3 separate dopamine precursor depletion studies [18, 56, 57]. The protocol, acquisition site, scanner and sequence were identical across the 3 studies. Participants with a history of drug abuse, neurological or psychiatric disorder were excluded. Informed consent was obtained from all participants.

Dopamine depletion

The acute phenylalanine and tyrosine depletion (APTD) technique [42, 48, 59] was used to reduce dopamine synthesis in healthy participants, following the procedure described previously [18, 56, 57]. It should be noted that although APTD leads to depletion of dopamine precursors and only reduces the dopamine synthesis and availability, the term *"dopamine depletion"* is used throughout this manuscript to refer to *"dopamine precursor depletion"* and APTD. Although APTD might also decrease norepinephrine synthesis, it has been shown that the release of norepinephrine is not affected under resting state conditions [39, 47]

Data acquisition and preprocessing

High-resolution, T1-weighted, three-dimensional structural MRIs were acquired for anatomical localization (1-mm^3 voxel size), as well as two resting-state echoplanar T2*-weighted images with blood oxygenation level-dependent (BOLD) contrast (3.5-mm isotropic voxels, TE 30 ms, TR 2 s, flip angle 90°) from all participants using a Siemens MAGNETOM Trio 3T MRI system at the Montréal Neurological Institute (MNI) in Montréal, Canada. Each participant was scanned for 5 minutes (150 vol) with eyes open, on two separate days, once following administration of a nutritionally balanced amino acid mixture (BAL) and once following acute phenylalanine/tyrosine depletion (APTD). The resting state fMRI data was preprocessed through the following steps: slice timing correction, rigid body motion correction, removal of slow temporal drift using a high-pass filter with 0.01 Hz cut-off, physiological noise correction, and motion correction using motion parameters. All preprocessing steps were performed using the Neuroimaging Analysis Kit (NIAK) [5, 6].

Anatomical MRI data was parcelled into 83 cortical and subcortical areas using the Desikan-Killiany atlas [22], and then further subdivided into 129, 234, 463 and 1015 approximately equally sized parcels following the procedure described by Cammoun and colleagues [15]. The parcellations were used to extract BOLD time series from functional MRI data. The time series of each parcel were estimated as the mean of all voxels in that parcel. All analyses were repeated at each resolution to ensure that none of the conclusions were idiosyncratic to a particular spatial scale.

Sample entropy

Sample entropy (SE) analysis was used to estimate regional signal variability [62]. The algorithm quantifies the conditional probability that any two sequences of time points with length of $m + 1$ will be similar to each other, given that the first m points of these sequences were similar (Figure S1). SE is then measured as the natural logarithm of this quantity, such that large values are assigned to unpredictable signals, and small values to predictable signals. The algorithm is subject to two pa-

rameters: the pattern length (m), which determines the segment length used to find repeating patterns, and the similarity criterion (r), which is the tolerance for accepting matches in the time series. The sample entropy of a time series with length N is estimated as

$$\mathrm{SE}(m, r, N) = \ln \frac{\sum_{i=1}^{N-m} n_i^m}{\sum_{i=1}^{N-m} n_i^{m+1}} \tag{1}$$

where n_i^m is the number of m-length segment of time series (e.g. segment j with length m) that are similar to the m-length segment i within to the similarity criterion, excluding self-matches ($i \neq j$; i.e., the algorithm does not compare patterns with themselves) [17].

Following the optimization proposed by Small & Tse [75], we set $m = 2$ as the pattern length. We set the similarity criterion to $r = 0.5$ times the standard deviation (SD) of the time series following the method proposed by Richman & Moorman [62]. Although these values of m and r have been used extensively in previous reports [4, 35, 44, 50], we sought to ensure that the reported results were robust across multiple choices of m and r. We therefore re-calculated SE using different values for m and r and re-ran the PLS analysis described below (see *Statistical assessment*). Figure S3 shows the correlation between new bootstrap ratios (i.e., changes in signal variability) with bootstrap ratios that were originally estimated by setting $m = 2$ and $r = 0.5 \times SD$. The correlations were generally greater than 0.7 across a range of similarity criteria r, and greater than 0.3 across a range of pattern lengths m, suggesting that the results were relatively insensitive to choice of parameters.

Statistical assessment

We used partial least squares (PLS) analysis to investigate changes in signal variability following the BAL vs. APTD conditions. PLS analysis is a multivariate statistical technique that is used to analyze two "blocks" or sets of variables [45, 46]. In neuroimaging studies, one set may represent neural activity, while the other may represent behaviour or experimental design (e.g. condition and/or group assignments). PLS analysis seeks to relate these two data blocks by constructing linear combinations of the original variables such that the new latent variables have maximum covariance [37].

In the present report, one block ($\mathbf{X}$) corresponded to regional signal variability estimated by sample entropy of BOLD time series. The rows of matrix $\mathbf{X}$ correspond to observations (participants nested within conditions) and the columns correspond to variables (regional signal variability). For p participants, c conditions, and v variables, matrix $\mathbf{X}$ will have $p \times c$ rows and v columns. Within-condition means are computed for each column and centered to give the matrix $\mathbf{M}$. Singular value decomposition (SVD) is applied to $\mathbf{M}$

$$\mathbf{USV}' = \mathbf{M} \tag{2}$$

resulting in a set of orthonormal left singular vectors, $\mathbf{U}$ and right singular vectors, $\mathbf{V}$, and a diagonal matrix of singular values, $\mathbf{S}$. The number of latent variables is equal to the rank of the mean-centered matrix (here c), so $\mathbf{U}$ will have c columns and v rows, and $\mathbf{V}$ and $\mathbf{S}$ will both have c columns and c rows.

The decomposition results in a set of latent variables that are composed of columns of singular vectors, $\mathbf{U}$ and $\mathbf{V}$, and a set of singular values from the diagonal matrix of $\mathbf{S}$. In the present study, the v elements of column vectors of $\mathbf{U}$ are the weights of original brain activity variables (i.e., signal variability) that contribute to the latent variable and demonstrate a pattern of changes in signal variability following dopamine depletion. The c elements of column vectors of $\mathbf{V}$ are the weights of experimental design variables that contribute to the same latent variable and are interpreted as a contrast between experimental conditions. The latent variables are mutually orthogonal and express the shared information between the two data blocks with maximum covariance. This covariance is reflected in the singular values from the diagonal elements of matrix $\mathbf{S}$ that are associated with each given latent variable.

We assessed the statistical significance of each latent variable using permutation tests [24]. During each permutation, the rows of matrix $\mathbf{X}$ were reordered randomly, destroying the condition assignment of each row. The new permuted data matrices were then mean-centered and subjected to SVD as before. The procedure was repeated 10,000 times to generate a distribution of singular values under the null hypothesis that there is no relationship between neural activity and study design. A p-value was estimated for each latent variable as the proportion of permuted singular values greater than or equal to the original singular value.

We assessed the reliability of singular vector weights using bootstrap resampling. Here, the rows of data matrix $\mathbf{X}$ were randomly resampled with replacement while keeping the original condition assignments. Mean-centering and SVD were then applied to the resampled data matrices as before. The results were used to build a sampling distribution for each weight in the singular vectors $\mathbf{U}$ and $\mathbf{V}$. A "bootstrap ratio" was then calculated for each original variable (i.e., for each node) as the ratio of the singular vector weight to its bootstrap-estimated standard error. Bootstrap ratios are designed to be large for variables that have a large weight (i.e., large contribution) as well as a small standard error (i.e., are stable). Bootstrap ratios are equivalent to z-scores if the bootstrap distribution is approximately unit normal [25]. In this case, 95% and 99% confidence intervals correspond to bootstrap ratios of ± 1.96 and ± 2.58, respectively.

Community detection

Functional networks were partitioned into communities or intrinsic networks using the assignment derived in [52], which we describe below. As we show in the *Results* section, the main conclusions also hold for the partitions reported by Yeo and colleagues [78] and Power and colleagues [60].

A Louvain-like greedy algorithm was used to identify a community assignment that maximized the quality function, Q [58, 65]

$$Q(\gamma) = \frac{1}{m^+}\sum_{ij}(W_{ij}^+ - \gamma p_{ij}^+)\delta(\sigma_i,\sigma_j) - \frac{1}{m^+ + m^-}\sum_{ij}(W_{ij}^- - \gamma p_{ij}^-)\delta(\sigma_i,\sigma_j) \quad (3)$$

where W_{ij}^+ and W_{ij}^- are the functional connectivity (correlation) matrices that contain only positive and only negative coefficients of correlation, respectively. $p_{ij}^\pm$ is the expected density of only positive or only negative connectivity matrices according to the configuration null model and is given as $p_{ij}^\pm = (s_i^\pm s_j^\pm)/2m^\pm$. $m^\pm = \sum_{i,j>i} W_{ij}^\pm$ is the total weight of all positive or negative connections of $W_{ij}^\pm$ (note that the summation is taken over $i, j > i$ to ensure that each connection is only counted once). The total weights of positive or negative connections of i and j are given by $s_i^\pm = \sum_i W_{ij}^\pm$ and $s_j^\pm = \sum_j W_{ij}^\pm$, respectively. The resolution parameter γ scales the importance of the null model and effectively controls the size of the detected communities: larger communities are more likely to be detected when $\gamma < 1$ and smaller communities (with fewer nodes in each community) are more likely to be detected when $\gamma > 1$. Furthermore, σ_i defines the community assignment of node i. The Kronecker function $\delta(\sigma_i, \sigma_j)$ is equal to 1 if $\sigma_i = \sigma_j$ and is equal to zero otherwise ($\sigma_i \neq \sigma_j$), ensuring that only within-community connections contribute to Q.

Multiple resolutions γ were assessed, from 0.5 to 10 in steps of 0.1. The Louvain algorithm was repeated 250 times for each γ value [10]. The resolution $\gamma = 1.5$ was chosen based on the similarity measures (Rand index) of pairs of partitions for each γ value, such that the similarity measures of a more stable set of partitions for a given γ value would have a larger mean and smaller standard deviation compared to similarity measures at other γ values (i.e., larger z-score of similarity measure) [77]. Finally, a consensus partition was found from the 250 partitions at $\gamma = 1.5$ following the method described in [2]. Eight communities or networks were detected, including visual (VIS), temporal (TEM), default mode (DMN), dorsal attention (DA), ventral attention (VA), somatomotor (SM) and salience (SAL) [52].

Cohesion and integration

Connectivity between and within modules was assessed as the participation coefficient and within-module degree z-score [33], using Brain Connectivity Toolbox (BCT) [64]. The participation coefficient quantifies how evenly distributed a node's connections are to all modules. Values close to 1 indicate that a node is connected to many communities, while values close to 0 indicate that a node is connected to few communities. The participation coefficient of node i, P_i, is given by:

$$P_i = 1 - \sum_{m\in M}\left(\frac{k_i(m)}{k_i}\right)^2 \quad (4)$$

where m is a module from a set of modules M, k_i is the weighted degree (i.e., connection strength) of node i, and $k_i(m)$ is the number of connections between node i and all other nodes in module m [33, 64]. To find participation coefficients of resting state networks, we first found the average participation coefficient of each node across all subjects and then compared the participation coefficients of the nodes that belong to the same module following the BAL vs. APTD conditions, using one-tailed Wilcoxon rank sum test.

The within-module degree is estimated as the weighted degree (i.e., strength) of the connections that node i makes to other nodes within the same module. The measure is then z-scored, expressing a node's weighted degree in terms of standard deviations above or below the mean degree of the nodes in the given module (Z_i). A positive within-module degree z-score indicates that a node is highly connected to other nodes within the same module, while a negative within-module z-score indicates a node participates in less than average connections within its own module. We estimated the within-module degree z-score of each node for each subject and then calculated the average Z_i over all subjects. Finally, we used one-tailed Wilcoxon rank sum test to compare the within-module degree z-scores of the nodes of a given module following the BAL and APTD conditions.

ACKNOWLEDGMENTS

BM acknowledges support from the Natural Sciences and Engineering Research Council of Canada (NSERC Discovery Grant RGPIN #017-04265) and from the Fonds de recherche du Québec - Santé (Chercheur Boursier). GS acknowledges support from the Healthy Brains for Healthy Lives (HBHL) initiative at McGill University. The authors gratefully acknowledge code from Dr. Richard F. Betzel (University of Pennsylvania, PA, USA) to create the boxplot figures.

AUTHOR CONTRIBUTIONS

Conceptualization, G.S., B.M. and A.D.; Methodology and Resources, C.A.C, J.T.C., A.N.-S., M.L., A.D.; Data Curation, Y.Z.; Formal Analysis and Investigation, G.S., Y.Z.; Writing-Original Draft, G.S., B.M. and A.D.; Writing-Review & Editing, G.S., Y.Z., M.L., B.M. and A.D.; Funding Acquisition, M.L., A.D. and B.M.

DECLARATION OF INTERESTS

The authors declare no competing interests.

[1] Barttfeld, P., Uhrig, L., Sitt, J. D., Sigman, M., Jarraya, B., and Dehaene, S. (2015). Signature of consciousness in the dynamics of resting-state brain activity. *Proc Natl Acad Sci USA*, 112(3):887–892.

[2] Bassett, D. S., Porter, M. A., Wymbs, N. F., Grafton, S. T., Carlson, J. M., and Mucha, P. J. (2013). Robust detection of dynamic community structure in networks. *Chaos: An Interdisciplinary Journal of Nonlinear Science*, 23(1):013142.

[3] Bassett, D. S., Yang, M., Wymbs, N. F., and Grafton, S. T. (2015). Learning-induced autonomy of sensorimotor systems. *Nat Neurosci*, 18(5):744–751.

[4] Beharelle, A. R., Kovačević, N., McIntosh, A. R., and Levine, B. (2012). Brain signal variability relates to stability of behavior after recovery from diffuse brain injury. *NeuroImage*, 60(2):1528–1537.

[5] Bellec, P., Lavoie-Courchesne, S., Dickinson, P., Lerch, J. P., Zijdenbos, A. P., and Evans, A. C. (2012). The pipeline system for octave and matlab (psom): a lightweight scripting framework and execution engine for scientific workflows. *Frontiers in neuroinformatics*, 6.

[6] Bellec, P., Rosa-Neto, P., Lyttelton, O. C., Benali, H., and Evans, A. C. (2010). Multi-level bootstrap analysis of stable clusters in resting-state fmri. *Neuroimage*, 51(3):1126–1139.

[7] Bertrand, J.-A., McIntosh, A. R., Postuma, R. B., Kovacevic, N., Latreille, V., Panisset, M., Chouinard, S., and Gagnon, J.-F. (2016). Brain connectivity alterations are associated with the development of dementia in parkinson's disease. *Brain Conn*, 6(3):216–224.

[8] Betzel, R. F., Fukushima, M., He, Y., Zuo, X.-N., and Sporns, O. (2016). Dynamic fluctuations coincide with periods of high and low modularity in resting-state functional brain networks. *NeuroImage*, 127:287–297.

[9] Björklund, A. and Dunnett, S. B. (2007). Fifty years of dopamine research. *Trends in Neurosciences*, 30(5):185 – 187.

[10] Blondel, V. D., Guillaume, J.-L., Lambiotte, R., and Lefebvre, E. (2008). Fast unfolding of communities in large networks. *Journal of Statistical Mechanics: Theory and Experiment*, 2008(10):P10008.

[11] Bolt, T., Prince, E. B., Nomi, J. S., Messinger, D., Llabre, M. M., and Uddin, L. Q. (2018). Combining region-and network-level brain-behavior relationships in a structural equation model. *NeuroImage*, 165:158–169.

[12] Braun, U., Schäfer, A., Walter, H., Erk, S., Romanczuk-Seiferth, N., Haddad, L., Schweiger, J. I., Grimm, O., Heinz, A., Tost, H., et al. (2015). Dynamic reconfiguration of frontal brain networks during executive cognition in humans. *Proc Natl Acad Sci USA*, 112(37):11678–11683.

[13] Cabral, J., Hugues, E., Sporns, O., and Deco, G. (2011). Role of local network oscillations in resting-state functional connectivity. *Neuroimage*, 57(1):130–139.

[14] Calhoun, V. D., Miller, R., Pearlson, G., and Adalı, T. (2014). The chronnectome: time-varying connectivity networks as the next frontier in fmri data discovery. *Neuron*, 84(2):262–274.

[15] Cammoun, L., Gigandet, X., Meskaldji, D., Thiran, J. P., Sporns, O., Do, K. Q., Maeder, P., Meuli, R., and Hagmann, P. (2012). Mapping the human connectome at multiple scales with diffusion spectrum mri. *J Meth*, 203(2):386–397.

[16] Carbonell, F., Nagano-Saito, A., Leyton, M., Cisek, P., Benkelfat, C., He, Y., and Dagher, A. (2014). Dopamine precursor depletion impairs structure and efficiency of resting state brain functional networks. *Neuropharmacology*, 84:90 – 100.

[17] Costa, M., Goldberger, A. L., and Peng, C.-K. (2005). Multiscale entropy analysis of biological signals. *Phys. Rev. E*, 71:021906.

[18] Coull, J. T., Hwang, H. J., Leyton, M., and Dagher, A. (2012). Dopamine precursor depletion impairs timing in healthy volunteers by attenuating activity in putamen and supplementary motor area. *Journal of Neuroscience*, 32(47):16704–16715.

[19] Cox, S. M., Frank, M. J., Larcher, K., Fellows, L. K., Clark, C. A., Leyton, M., and Dagher, A. (2015). Striatal d1 and d2 signaling differentially predict learning from positive and negative outcomes. *Neuroimage*, 109:95–101.

[20] Deco, G., Jirsa, V. K., and McIntosh, A. R. (2010). Emerging concepts for the dynamical organization of resting-state activity in the brain. *Nat Rev Neurosci*, 12(1):nrn2961.

[21] del Campo, N., Fryer, T. D., Hong, Y. T., Smith, R., Brichard, L., Acosta-Cabronero, J., Chamberlain, S. R., Tait, R., Izquierdo, D., Regenthal, R., et al. (2013). A positron emission tomography study of nigro-striatal dopaminergic mechanisms underlying attention: implications for adhd and its treatment. *Brain*, 136(11):3252–3270.

[22] Desikan, R. S., Ségonne, F., Fischl, B., Quinn, B. T., Dickerson, B. C., Blacker, D., Buckner, R. L., Dale, A. M., Maguire, R. P., Hyman, B. T., Albert, M. S., and Killiany, R. J. (2006). An automated labeling system for subdividing the human cerebral cortex on mri scans into gyral based regions of interest. *NeuroImage*, 31(3):968 – 980.

[23] Durstewitz, D., Seamans, J. K., and Sejnowski, T. J. (2000). Dopamine-mediated stabilization of delay-period activity in a network model of prefrontal cortex. *J Neurophysiol*, 83(3):1733–1750.

[24] Edgington, E. and Onghena, P. (2007). *Randomization tests*. CRC Press.

[25] Efron, B. and Tibshirani, R. (1986). Bootstrap methods for standard errors, confidence intervals, and other measures of statistical accuracy. *Statist. Sci.*, 1(1):54 – 75.

[26] Fries, P. (2005). A mechanism for cognitive dynamics: neuronal communication through neuronal coherence. *Trends Cogn Sci*, 9(10):474–480.

[27] Garrett, D. D., Kovacevic, N., McIntosh, A. R., and Grady, C. L. (2011). The importance of being variable. *J Neurosci*, 31(12):4496–4503.

[28] Garrett, D. D., McIntosh, A. R., and Grady, C. L. (2013a). Brain signal variability is parametrically modifiable. *Cerebral Cortex*, 24(11):2931–2940.

[29] Garrett, D. D., Samanez-Larkin, G. R., MacDonald, S. W., Lindenberger, U., McIntosh, A. R., and Grady, C. L. (2013b). Moment-to-moment brain signal variability: A next frontier in human brain mapping? *Neuroscience & Biobehavioral Reviews*, 37(4):610–624.

[30] Gilat, M., Bell, P. T., Martens, K. A. E., Georgiades, M. J., Hall, J. M., Walton, C. C., Lewis, S. J., and Shine, J. M. (2017). Dopamine depletion impairs gait automaticity by altering cortico-striatal and cerebellar processing in parkinson's disease. *NeuroImage*, 152:207–220.

[31] Godwin, D., Barry, R. L., and Marois, R. (2015). Breakdown of the brain's functional network modularity with awareness. *Proc Natl Acad Sci USA*, 112(12):3799–3804.

[32] Goto, Y., Otani, S., and Grace, A. A. (2007). The yin and yang of dopamine release: a new perspective. *Neuropharmacology*, 53(5):583–587.

[33] Guimerà, R. and Amaral, L. A. N. (2005). Cartography of complex networks: modules and universal roles. *Journal of Statistical Mechanics: Theory and Experiment*, 2005(02):P02001.

[34] Guitart-Masip, M., Salami, A., Garrett, D., Rieckmann, A., Lindenberger, U., and Bäckman, L. (2015). Bold variability is related to dopaminergic neurotransmission and cognitive aging. *Cereb Cortex*, 26(5):2074–2083.

[35] Heisz, J. J., Shedden, J. M., and McIntosh, A. R. (2012). Relating brain signal variability to knowledge representation. *NeuroImage*, 63(3):1384–1392.

[36] Kitzbichler, M. G., Henson, R. N., Smith, M. L., Nathan, P. J., and Bullmore, E. T. (2011). Cognitive effort drives workspace configuration of human brain functional networks. *J Neurosci*, 31(22):8259–8270.

[37] Krishnan, A., Williams, L. J., McIntosh, A. R., and Abdi, H. (2011). Partial least squares (pls) methods for neuroimaging: A tutorial and review. *NeuroImage*, 56(2):455 – 475.

[38] Kroener, S., Chandler, L. J., Phillips, P. E., and Seamans, J. K. (2009). Dopamine modulates persistent synaptic activity and enhances the signal-to-noise ratio in the prefrontal cortex. *PLoS ONE*, 4(8):e6507.

[39] Le Masurier, M., Zetterström, T., Cowen, P., and Sharp, T. (2014). Tyrosine-free amino acid mixtures reduce physiologically-evoked release of dopamine in a selective and activity-dependent manner. *Journal of Psychopharmacology*, 28(6):561–569.

[40] Lee, W. H. and Frangou, S. (2017). Linking functional connectivity and dynamic properties of resting-state networks. *Sci Rep*, 7(1):16610.

[41] Leyton, M., Dagher, A., Boileau, I., Casey, K., Baker, G. B., Diksic, M., Gunn, R., Young, S. N., and Benkelfat, C. (2004). Decreasing amphetamine-induced dopamine release by acute phenylalanine/tyrosine depletion: a pet/[11c] raclopride study in healthy men. *Neuropsychopharmacology*, 29(2):427.

[42] Leyton, M., Young, S. N., Pihl, R. O., Etezadi, S., Lauze, C., Blier, P., Baker, G. B., and Benkelfat, C. (2000). Effects on mood of acute phenylalanine/tyrosine depletion in healthy women. *Neuropsychopharmacology*, 22(1):52–63.

[43] McAuley, J. (2003). The physiological basis of clinical deficits in parkinson's disease. *Progress in Neurobiology*, 69(1):27 – 48.

[44] McIntosh, A. R., Kovacevic, N., and Itier, R. J. (2008). Increased brain signal variability accompanies lower behavioral variability in development. *PLoS Comput Biol*, 4(7):e1000106.

[45] McIntosh, A. R. and Lobaugh, N. J. (2004). Partial least squares analysis of neuroimaging data: applications and advances. *NeuroImage*, 23:S250 – S263.

[46] McIntosh, A. R. and Mišić, B. (2013). Multivariate statistical analyses for neuroimaging data. *Annual Review of Psychology*, 64(1):499–525.

[47] McTavish, S. F., Cowen, P. J., and Sharp, T. (1999a). Effect of a tyrosine-free amino acid mixture on regional brain catecholamine synthesis and release. *Psychopharmacology*, 141(2):182–188.

[48] McTavish, S. F. B., McPherson, M. H., Sharp, T., and Cowen, P. J. (1999b). Attenuation of some subjective effects of amphetamine following tyrosine depletion. *Journal of Psychopharmacology*, 13(2):144–147.

[49] Mišic, B., Doesburg, S. M., Fatima, Z., Vidal, J., Vakorin, V. A., Taylor, M. J., and McIntosh, A. R. (2015). Coordinated information generation and mental flexibility: large-scale network disruption in children with autism. *Cereb Cortex*, 25(9):2815–2827.

[50] Mišić, B., Dunkley, B. T., Sedge, P. A., Da Costa, L., Fatima, Z., Berman, M. G., Doesburg, S. M., McIntosh, A. R., Grodecki, R., Jetly, R., et al. (2016). Posttraumatic stress constrains the dynamic repertoire of neural activity. *J Neurosci*, 36(2):419–431.

[51] Mišić, B., Mills, T., Taylor, M. J., and McIntosh, A. R. (2010). Brain noise is task dependent and region specific. *J Neurophysiol*, 104(5):2667–2676.

[52] Mišić, B., Betzel, R. F., Nematzadeh, A., Goñi, J., Griffa, A., Hagmann, P., Flammini, A., Ahn, Y.-Y., and Sporns, O. (2015). Cooperative and competitive spreading dynamics on the human connectome. *Neuron*, 86(6):1518 – 1529.

[53] Mohr, H., Wolfensteller, U., Betzel, R. F., Mišić, B., Sporns, O., Richiardi, J., and Ruge, H. (2016). Integration and segregation of large-scale brain networks during short-term task automatization. *Nat Commun*, 7:13217.

[54] Mohr, P. N. and Nagel, I. E. (2010). Variability in brain activity as an individual difference measure in neuroscience? *J Neurosci*, 30(23):7755–7757.

[55] Montgomery, A. J., McTavish, S. F., Cowen, P. J., and Grasby, P. M. (2003). Reduction of brain dopamine concentration with dietary tyrosine plus phenylalanine depletion: an [11c] raclopride pet study. *American Journal of Psychiatry*, 160(10):1887–1889.

[56] Nagano-Saito, A., Cisek, P., Perna, A. S., Shirdel, F. Z., Benkelfat, C., Leyton, M., and Dagher, A. (2012). From

anticipation to action, the role of dopamine in perceptual decision making: an fmri-tyrosine depletion study. *Journal of Neurophysiology*, 108(2):501–512.

[57] Nagano-Saito, A., Leyton, M., Monchi, O., Goldberg, Y. K., He, Y., and Dagher, A. (2008). Dopamine depletion impairs frontostriatal functional connectivity during a set-shifting task. *Journal of Neuroscience*, 28(14):3697–3706.

[58] Newman, M. E. J. and Girvan, M. (2004). Finding and evaluating community structure in networks. *Phys. Rev. E*, 69:026113.

[59] Palmour, R. M., Ervin, F. R., Baker, G. B., and Young, S. N. (1998). An amino acid mixture deficient in phenylalanine and tyrosine reduces cerebrospinal fluid catecholamine metabolites and alcohol consumption in vervet monkeys. *Psychopharmacology*, 136(1):1–7.

[60] Power, J. D., Cohen, A. L., Nelson, S. M., Wig, G. S., Barnes, K. A., Church, J. A., Vogel, A. C., Laumann, T. O., Miezin, F. M., Schlaggar, B. L., and Petersen, S. E. (2011). Functional network organization of the human brain. *Neuron*, 72(4):665 – 678.

[61] Ramdani, C., Carbonnell, L., Vidal, F., Béranger, C., Dagher, A., and Hasbroucq, T. (2015). Dopamine precursors depletion impairs impulse control in healthy volunteers. *Psychopharmacology*, 232(2):477–487.

[62] Richman, J. S. and Moorman, J. R. (2000). Physiological time-series analysis using approximate entropy and sample entropy. *American Journal of Physiology-Heart and Circulatory Physiology*, 278(6):H2039–H2049.

[63] Roberts, J. A., Friston, K. J., and Breakspear, M. (2017). Clinical applications of stochastic dynamic models of the brain, part ii: A review. *Biol Psychiat*.

[64] Rubinov, M. and Sporns, O. (2010). Complex network measures of brain connectivity: Uses and interpretations. *NeuroImage*, 52(3):1059 – 1069.

[65] Rubinov, M. and Sporns, O. (2011). Weight-conserving characterization of complex functional brain networks. *NeuroImage*, 56(4):2068 – 2079.

[66] Samanez-Larkin, G. R., Kuhnen, C. M., Yoo, D. J., and Knutson, B. (2010). Variability in nucleus accumbens activity mediates age-related suboptimal financial risk taking. *J Neurosci*, 30(4):1426–1434.

[67] Schultz, W. (2002). Getting formal with dopamine and reward. *Neuron*, 36(2):241–263.

[68] Seamans, J. K. and Robbins, T. W. (2010). Dopamine modulation of the prefrontal cortex and cognitive function. In *The dopamine receptors*, pages 373–398.

[69] Seamans, J. K. and Yang, C. R. (2004). The principal features and mechanisms of dopamine modulation in the prefrontal cortex. *Prog Neurobiol*, 74(1):1–58.

[70] Shen, K., Hutchison, R. M., Bezgin, G., Everling, S., and McIntosh, A. R. (2015a). Network structure shapes spontaneous functional connectivity dynamics. *J Neurosci*, 35(14):5579–5588.

[71] Shen, K., Mišić, B., Cipollini, B. N., Bezgin, G., Buschkuehl, M., Hutchison, R. M., Jaeggi, S. M., Kross, E., Peltier, S. J., Everling, S., et al. (2015b). Stable long-range interhemispheric coordination is supported by direct anatomical projections. *Proc Natl Acad Sci USA*, 112(20):6473–6478.

[72] Shine, J., van den Brink, R., Hernaus, D., Nieuwenhuis, S., and Poldrack, R. (2017). Catecholaminergic manipulation alters dynamic network topology across behavioral states. *bioRxiv*, page 169102.

[73] Shine, J. M., Bissett, P. G., Bell, P. T., Koyejo, O., Balsters, J. H., Gorgolewski, K. J., Moodie, C. A., and Poldrack, R. A. (2016a). The dynamics of functional brain networks: Integrated network states during cognitive task performance. *Neuron*, 92(2):544–554.

[74] Shine, J. M., Koyejo, O., and Poldrack, R. A. (2016b). Temporal metastates are associated with differential patterns of time-resolved connectivity, network topology, and attention. *Proc Natl Acad Sci USA*, page 201604898.

[75] Small, M. and Tse, C. (2004). Optimal embedding parameters: a modelling paradigm. *Physica D: Nonlinear Phenomena*, 194(3):283 – 296.

[76] Surmeier, D. J., Carrillo-Reid, L., and Bargas, J. (2011). Dopaminergic modulation of striatal neurons, circuits, and assemblies. *Neuroscience*, 198:3–18.

[77] Traud, A. L., Kelsic, E. D., Mucha, P. J., and Porter, M. A. (2011). Comparing community structure to characteristics in online collegiate social networks. *SIAM Review*, 53(3):526–543.

[78] Yeo, B. T. T., Krienen, F. M., Sepulcre, J., Sabuncu, M. R., Lashkari, D., Hollinshead, M., Roffman, J. L., Smoller, J. W., Zöllei, L., Polimeni, J. R., Fischl, B., Liu, H., and Buckner, R. L. (2011). The organization of the human cerebral cortex estimated by intrinsic functional connectivity. *Journal of Neurophysiology*, 106(3):1125–1165.

[79] Zalesky, A., Fornito, A., Cocchi, L., Gollo, L. L., and Breakspear, M. (2014). Time-resolved resting-state brain networks. *Proc Natl Acad Sci USA*, 111(28):10341–10346.

[80] Zhang, J., Cheng, W., Liu, Z., Zhang, K., Lei, X., Yao, Y., Becker, B., Liu, Y., Kendrick, K. M., Lu, G., et al. (2016). Neural, electrophysiological and anatomical basis of brain-network variability and its characteristic changes in mental disorders. *Brain*, 139(8):2307–2321.

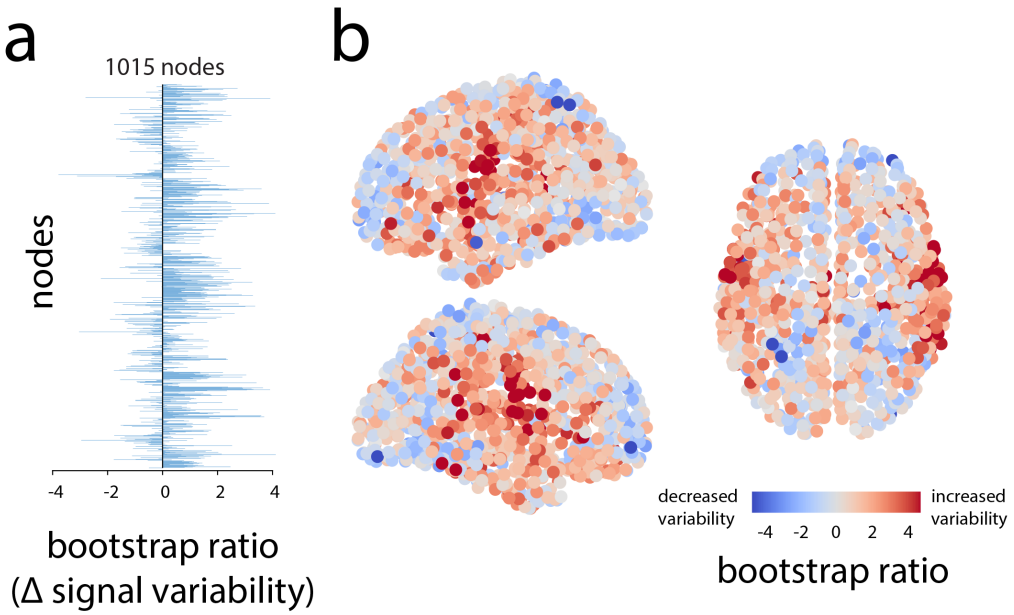

FIG. 1. **Dopamine depletion increases signal variability** | PLS analysis identified a contrast between patterns of signal variability in depletion (APTD) vs. non-depletion (BAL) conditions (permuted $p = 0.014$). The change in signal variability of each node is given by a bootstrap ratio for that node: such that a positive bootstrap ratio shows increase in signal variability of the node following dopamine depletion, while a negative bootstrap ratio shows the opposite. (a) Bootstrap ratios are depicted at the finest resolution (1015 nodes), showing that dopamine depletion increases signal variability at most nodes. (b) Boostrap ratios are shown in 3D space sagittally and axially. These corresponding results are shown for all resolutions in Fig. S2.

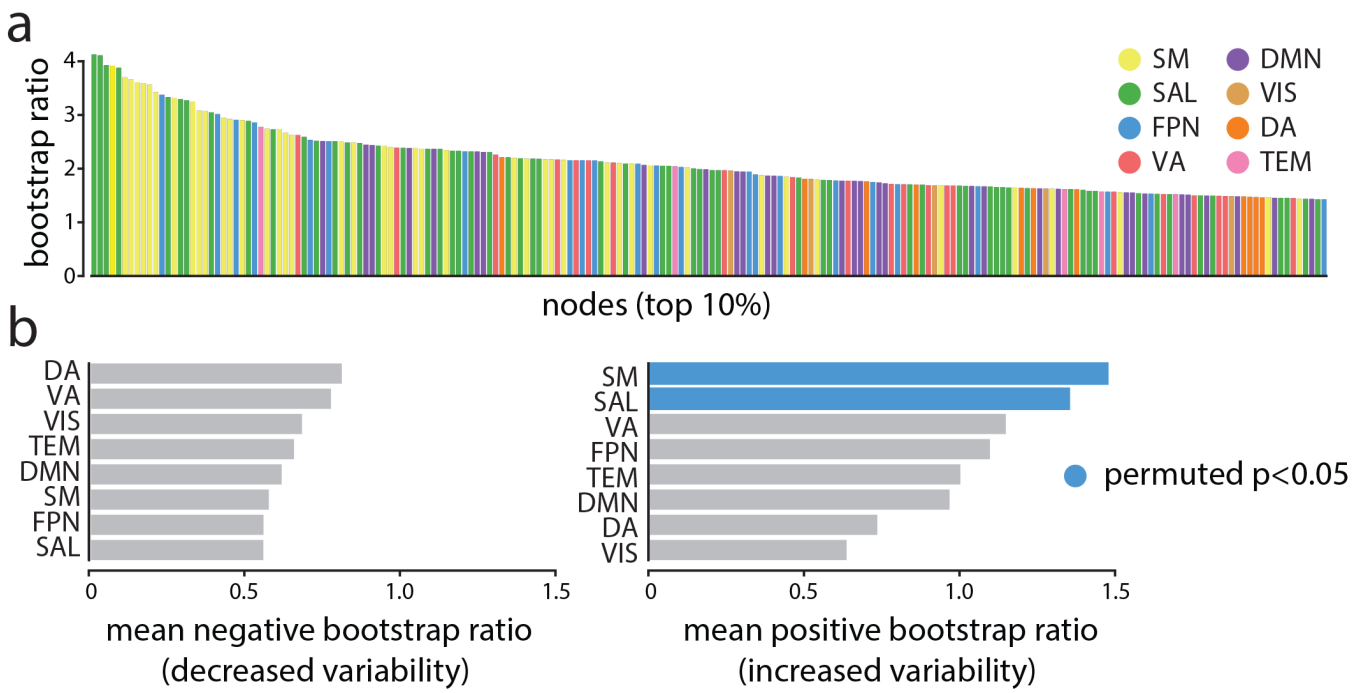

FIG. 2. **Node- and network-level effects of dopamine depletion** | (a) The top 10% of the nodes (i.e. top 100 nodes) that had the largest increase in signal variability (largest bootstrap ratios) following dopamine depletion. Each bar shows the magnitude of bootstrap ratio of a node and is colored based on the community assignment of that node [52]. Somatomotor (yellow) and salience (green) networks appear over-represented compared to other networks. (b) The mean changes in signal variability was calculated for each network and assessed by permutation tests (10,000 repetitions). Increases and decreases are shown separately. Signal variability increases most in the somatomotor and salience networks following dopamine depletion, and these are the only two networks where this effect is statistically significant. SM = somatomotor, SAL = salience, FPN = fronto-parietal, VA = ventral attention, DMN = default mode, VIS = visual, DA = dorsal attention, TEM = temporal.

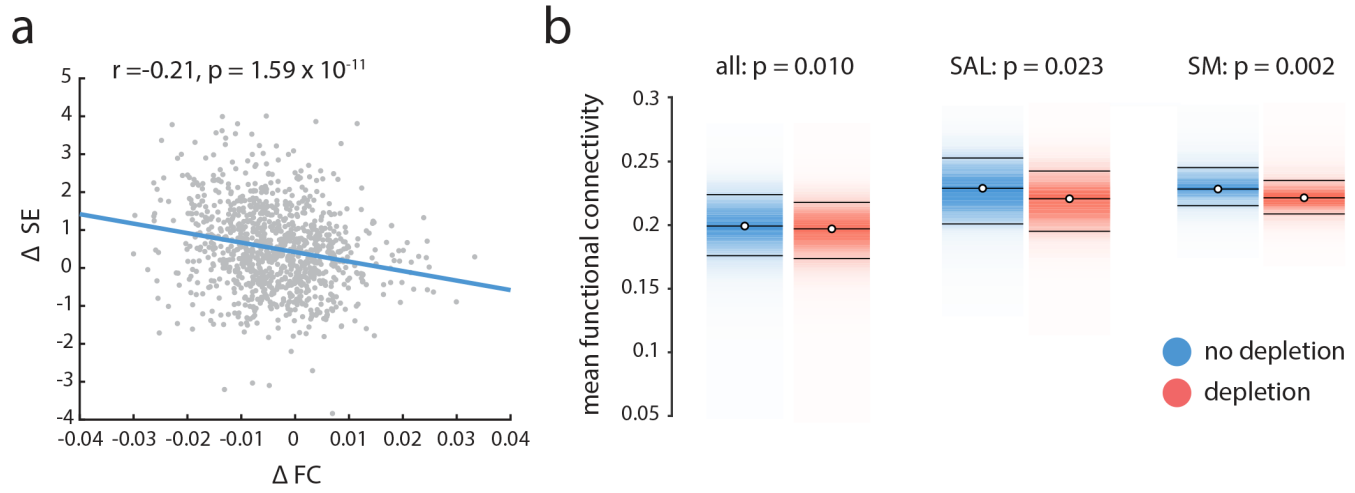

FIG. 3. **Relating signal variability and functional connectivity** | (a) Average changes in functional connectivity following dopamine depletion were estimated across all nodes and correlated with changes in signal variability. Changes in functional connectivity are related to changes in signal variability, such that the larger the increase in signal variability, the larger the decrease in functional connectivity. (b) Mean functional connectivity in depletion (APTD) vs. non-depletion (BAL) conditions, shown for all nodes (left) as well as only for nodes belonging to the somatomotor (SM) and salience (SAL) networks. Functional connectivity decreases in all instances (Wilcoxon rank sum test).

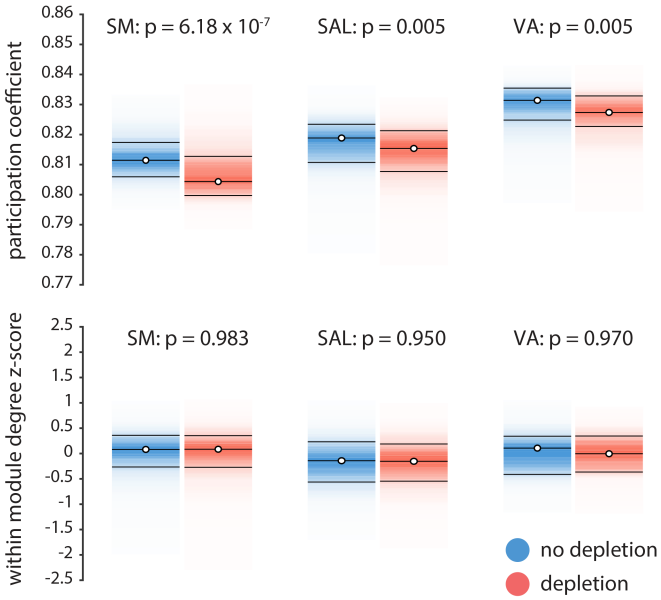

FIG. 4. **The effects of dopamine depletion on cohesion and diversity of specific intrinsic networks** | Mean participation coefficient significantly decreases in somatomotor (SM) , salience (SAL) and ventral attention (VA) networks after dopamine depletion (top row); however, within-module degree z-score remains unaffected (bottom row).

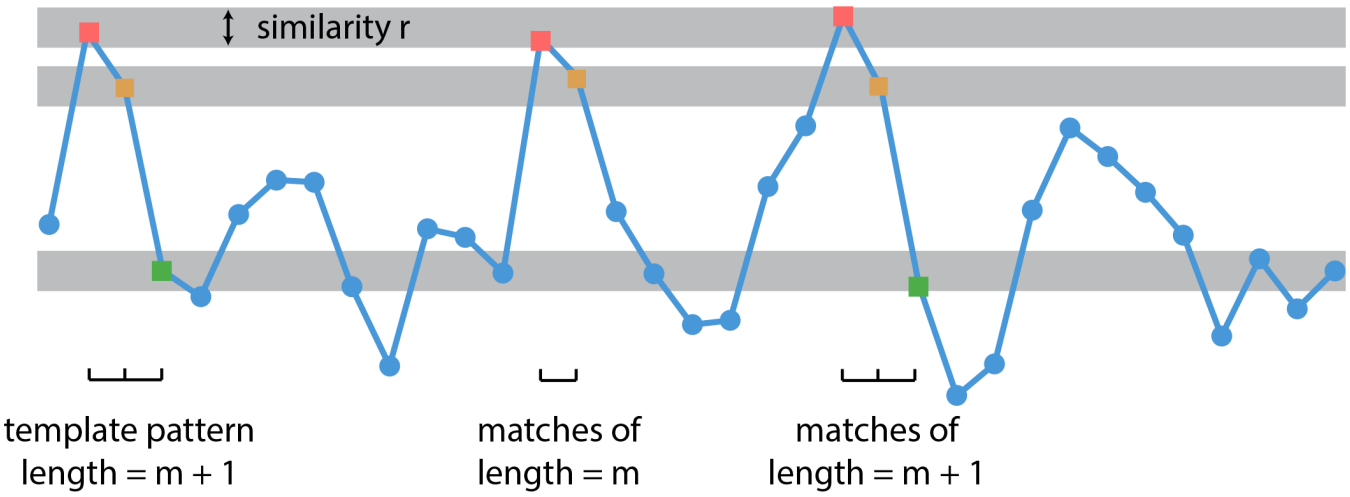

FIG. S1. **Sample entropy of a time series** | Signal variability is calculated using sample entropy analysis. Sample entropy measures the conditional probability that any two sequences of data points with length $m + 1$ will be similar to one another under the condition that they were similar for the first m points. The similarity criterion r represents the tolerance of algorithm to accept matches in the time series.

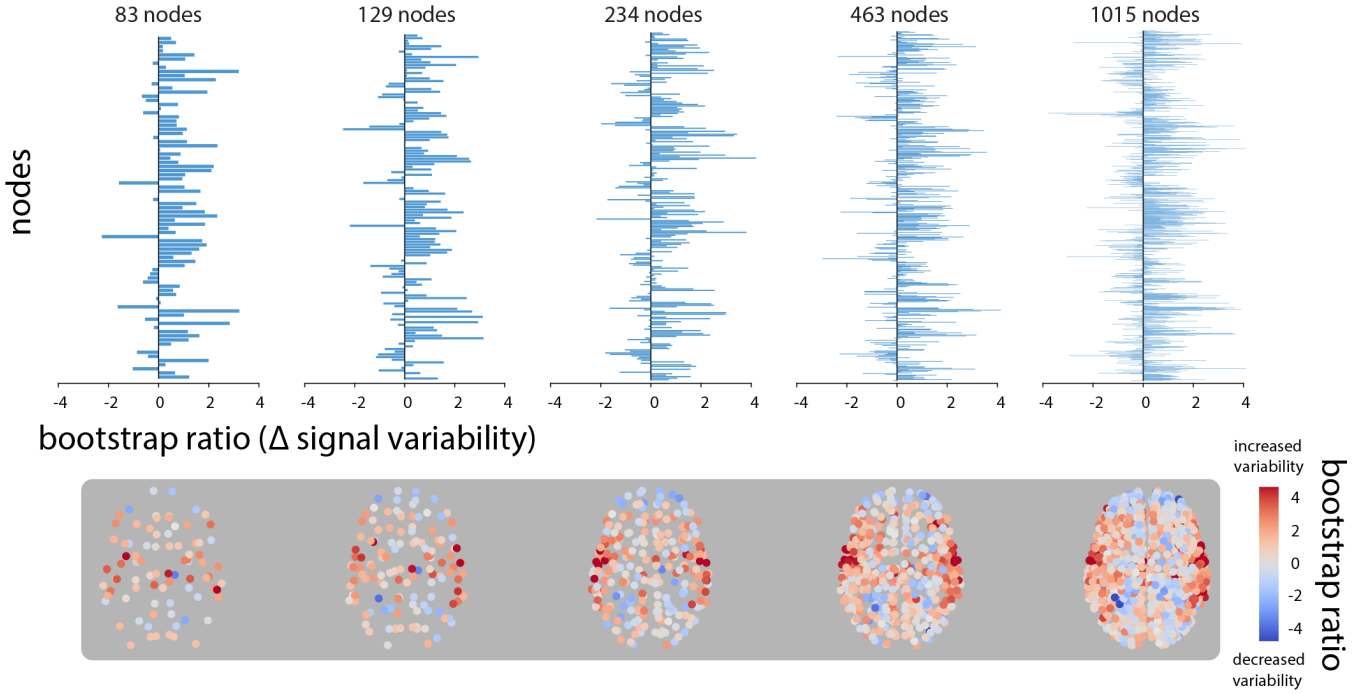

FIG. S2. **Replicating results using alternative parcellation resolutions |** In all parcellation resolutions, PLS analysis identifies a contrast between the patterns of signal variability in depletion (APTD) vs. non-depletion (BAL) conditions, (permuted p-values for the 5 resolutions from 83 nodes to 1015 nodes are as following: $p = 0.047$, $p = 0.023$, $p = 0.006$, $p = 0.013$, and $p = 0.014$). Changes in signal variability of each node is given by a bootstrap ratio for that node, such that a positive bootstrap ratio shows increased variability of the node following dopamine depletion, while a negative bootstrap ratio shows the opposite. The bootstrap ratios are depicted at all resolutions by bar graphs (first row) and on each node of the brain network (second row).

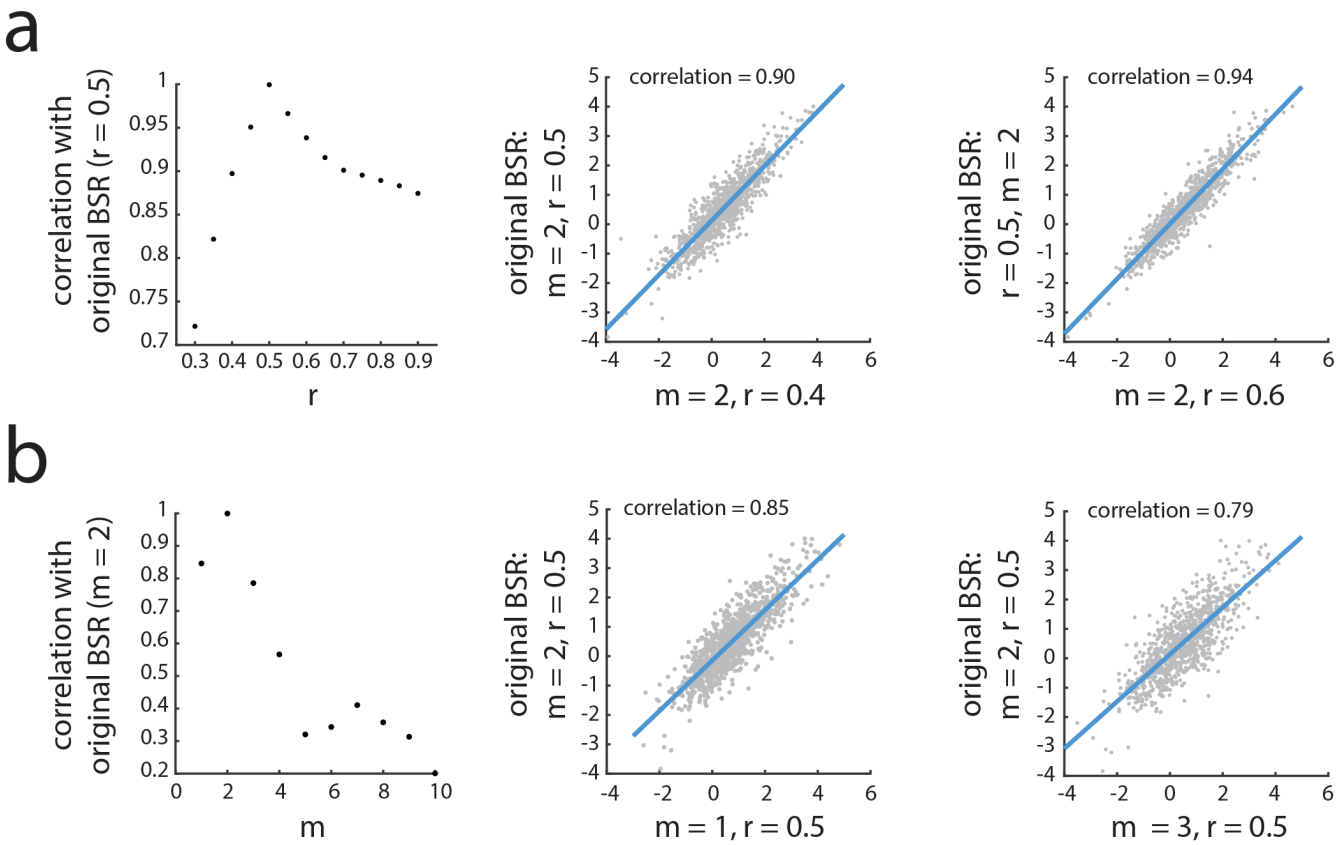

FIG. S3. **Choosing parameters for sample entropy analysis** | The whole analysis was repeated several times to ensure that results are not affected by the choice of parameters used to estimate signal variability. For this purpose, signal variability was calculated for various m and r values. Results of each m and r value were subjected to PLS analysis and new bootstrap ratios were estimated each time. (a) New bootstrap ratios estimated for varying similarity criterion, r, were correlated with original bootstrap ratios that were estimated with $r = 0.5 \times SD$. The correlation coefficient at each r is shown in this figure. Note that pattern length was kept constant as $m = 2$. The correlation of bootstrap ratios for $r = 0.4 \times SD$ and $r = 0.6 \times SD$ with the original bootstrap ratios ($r = 0.5 \times SD$) are shown as examples. (b) Keeping similarity criterion unchanged at $r = 0.5 \times SD$, the correlation coefficients of new bootstrap ratios for varying pattern length, m, with original bootstrap ratio with $m = 2$ were estimated. Correlation of bootstrap ratios for $m = 1$ and $m = 3$ with original bootstrap ratios ($m = 2$) are depicted to show examples of varying m.

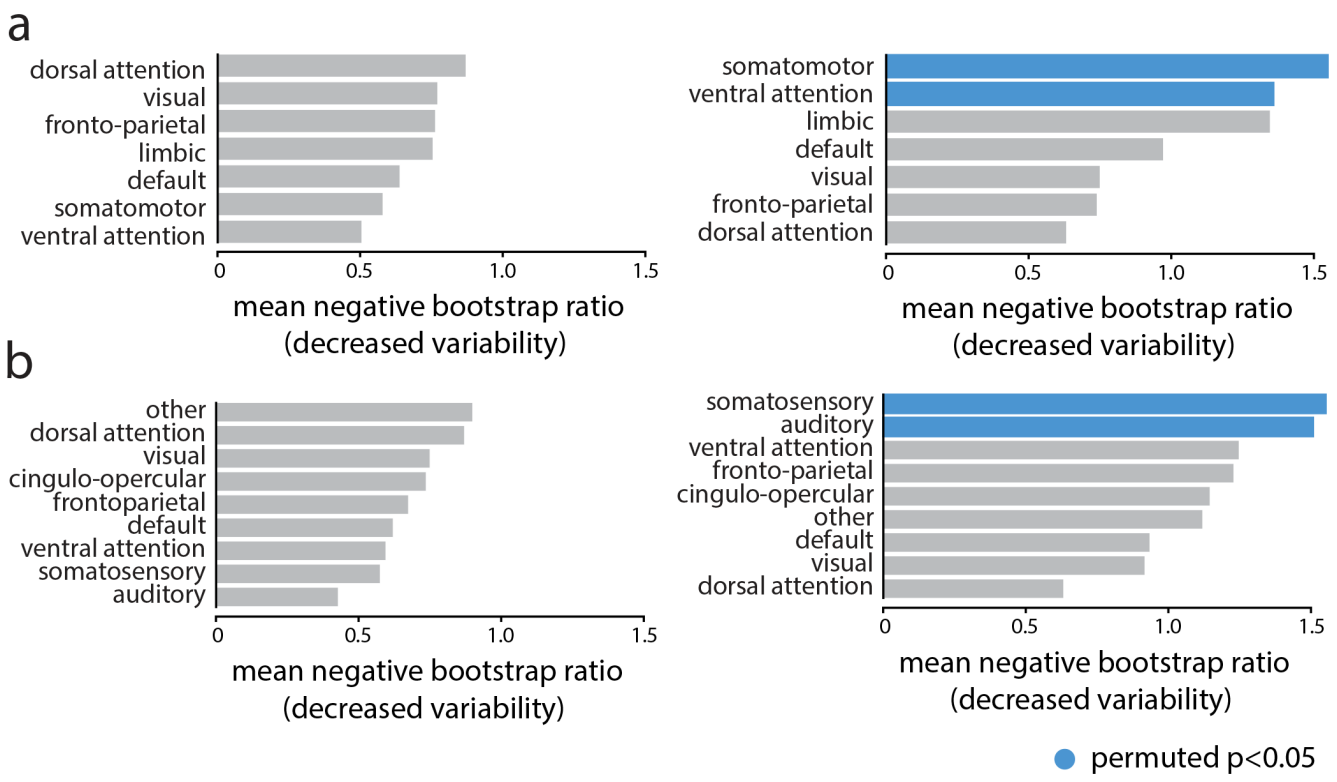

FIG. S4. **Replicating results using alternative network partitions** | Average signal variability was estimated at each resting state brain network using two of other well-known community assignments defined by Yeo and colleagues [78], and Power and colleagues [60]. The significance of the average signal variabilities in each network was determined by 10,000 permutation tests. The results are consistent with Figure 2, confirming that our analysis is independent from the methods used to identify community assignments.

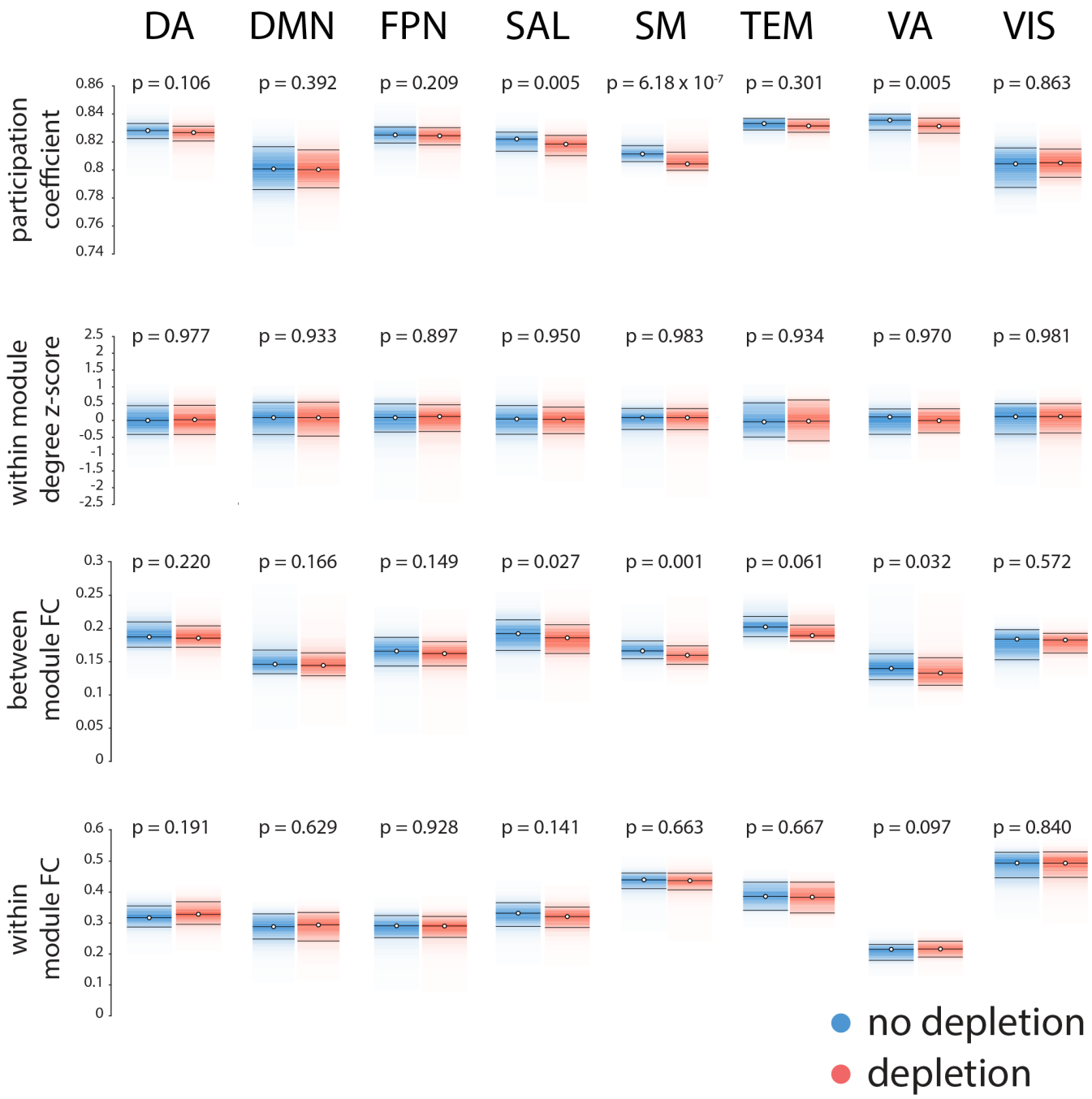

FIG. S5. **Replicating results using alternative measures of network cohesion and diversity** | In addition to the results shown in Figure 4, mean participation coefficient and within-module degree z-score were calculated in other intrinsic brain networks. Furthermore, average between- and within- module connectivity were investigated as additional measures of modular segregation. Confirming the results shown for participation coefficient and within-module degree z-score here and in Figure 4, the average between-module connectivity significantly decreases in somatomotor, salience and ventral attention networks following dopamine depletion whereas no significant change is observed in the average within-module connectivity.